05

Autowave description of the temperature effect during deformation of FCC metals

© L.B. Zuev, S.A. Barannikova, S.V. Kolosov

Institute of Strength Physics and Materials Science, Siberian Branch, Russian Academy of Sciences,
634055 Tomsk, Russia
e-mail: lbz@ispms.ru

Received June 28, 2022
Revised June 28, 2022
Accepted September 7, 2022

The data of comparative studies of the development of plastic flow in pure aluminum and iron-based austenitic alloy (Fe-Cr-Ni) are presented. Deformation patterns were studied during tests in the temperature range $143 \leq T \leq 420$ K. It was found that the effect of temperature is different for these two cases. When a stationary dissipative structure appears at the stage of parabolic strain hardening, the effect of temperature is determined by the change in the length of the localized plasticity autowave. At the stage of linear strain hardening, when a phase autowave of localized plasticity is formed, the effect is associated with an exponential increase in its rate with temperature.

Keywords: plastic deformation, localization, metals, Debye temperature.

DOI: 10.21883/TP.2022.12.55192.170-22

Introduction

Experimental studies and analysis of the kinetics of the solids plastic deformation development [1,2] shown that the essence of this process is the generation and regular evolution of a small set of autowave modes of macroscopically localized plastic flow, transforming into each other when the law of strain hardening changes during deformation. Autowave modes form the pattern of localized plasticity observed on the surface. It is generally characterized by its macroscopic space-time scales: length $\lambda \approx 10^{-2}$ m and time period $10^3 > T_t > 10^2$ s of autowave, as well as its propagation speed $10^{-5} \leq V_{aw} = \lambda/T_t \leq 10^{-4}$ m/s, depending on the strain-hardening coefficient and structure of the deformable material.

The dispersion law for autowaves of localized plasticity has the quadratic form $\omega_{aw}(k) \propto 1 + k^2$, where $\omega_{aw} = 2\pi/T_t$ is the autowave frequency, and $k = 2\pi/\lambda$ is the wavenumber [1]. This type of dispersion law indicates a significant nonlinearity of plastic flow processes.

As was established in experiments carried out on a wide range of plastic deformable materials (single- and polycrystals, metals and alloys, alkali-halide crystals and rocks), the autowave nature of the materials plastic deformation development is universal [1]. Evidence for the existence of autowave effects was obtained during mechanical tests under active loading and creep.

The main regularities of autowave processes of plastic flow are consequences of the elastic-plastic deformation invariant, which (for a phase autowave of localized plasticity) has the form [1,2]:

$$\frac{\lambda V_{aw}}{\chi V_t} = \hat{Z} \approx \frac{1}{2}. \qquad (1)$$

Equation (1), where χ is the interplanar distance, and V_t is the propagation speed of transverse ultrasonic waves, connects the parameters of autowave plastic deformation with the lattice characteristics of the material.

The aim of this paper was to analyze the temperature effect on the autowave mechanism of plasticity and to search for the nature of the relationship between the temperature behavior of the material plasticity characteristics and the parameters of autowave deformation processes at the stages of parabolic and linear strain hardening. It is known that stationary dissipative structures are generated on the first of them, and phase autowaves of localized plastic flow on the second one [1,2]. In both cases, the deformable medium turns out to be stratified into alternating deformable and non-deformable zones. The boundaries of such zones are immobile under parabolic, but move under linear strain hardening.

1. Materials and experimental procedure

In accordance with this task, in this paper polycrystalline FCC metals are used as materials: pure aluminum (Al content minimum 99.5 wt.%) with a grain size of $\sim 10.5\,\mu$ m (hereinafter — aluminum) and a multicomponent iron-based alloy (18 wt.% Cr–10 wt.% Ni) with a grain size $\sim 12.5\,\mu$m (hereinafter — austenite). This choice of materials is determined by the possibility of realizing in them under plastic deformation of stable stages of flow curves $\sigma(\varepsilon)$, determined by specific micromechanisms of plastic flow in these two materials [3].

Flat specimens with working part sizes $40 \times 5 \times 2$ mm were tensioned on a testing machine „Instron-1185“ at a speed of $3.3 \cdot 10^{-4}\,\mathrm{s}^{-1}$. The tests were carried out in the temperature range $143 \le T \le 420$ K. Such temperatures were achieved by purging the working chamber with nitrogen vapor from a Dewar vessel, the speed of which was controlled by a heating element located inside the Dewar vessel. The temperature of the sample was continuously monitored by a chromel-alumel thermocouple, the junction of which was in contact with it.

The deformation curves of aluminum and austenite in this temperature range have a complex multistage form. In order to identify the necessary stages of strain hardening, the initial indicating flow curves, recorded in the coordinates „stress σ – strain ε“, were rearranged into dependences „true stress s – true strain e“ (Fig. 1) and approximated by the Ludwik formula $s = s_0 + \vartheta e^n$ [3], where s_0 and ϑ — empirical constants. The straight sections of the graphs in the coordinates $\ln(s - s_0) - e^{1/2}$ or $\ln(s - s_0) - e$ were identified, as shown in Fig. 2, parabolic $(n = 0.5)$ stage in aluminium and linear $(n = 1)$ stage in austenite were determined.

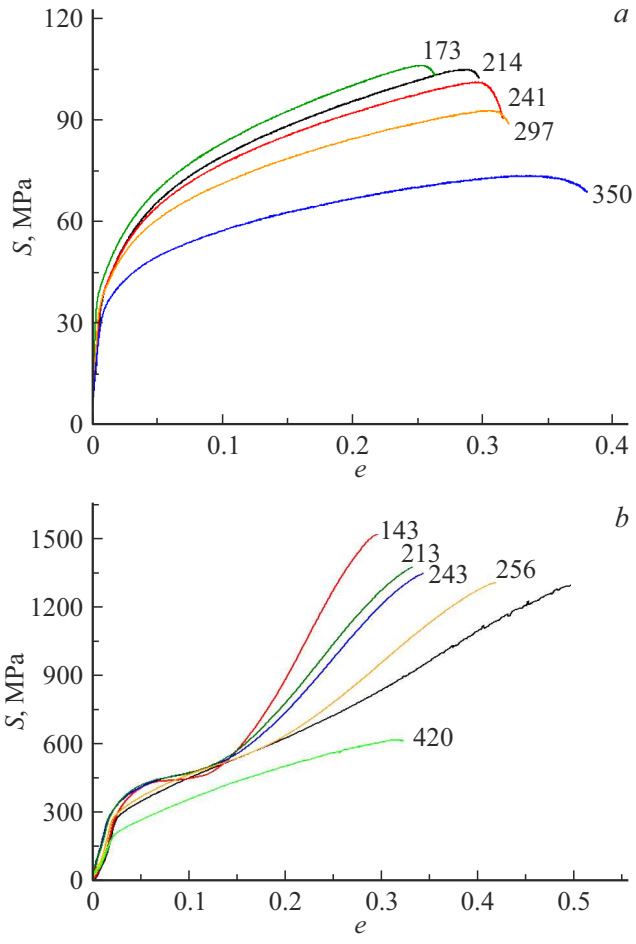

Figure 1. Plastic flow curves of aluminum (a) and austenite (b) at different test temperatures in true coordinates. Numbers near curves are test temperatures (K).

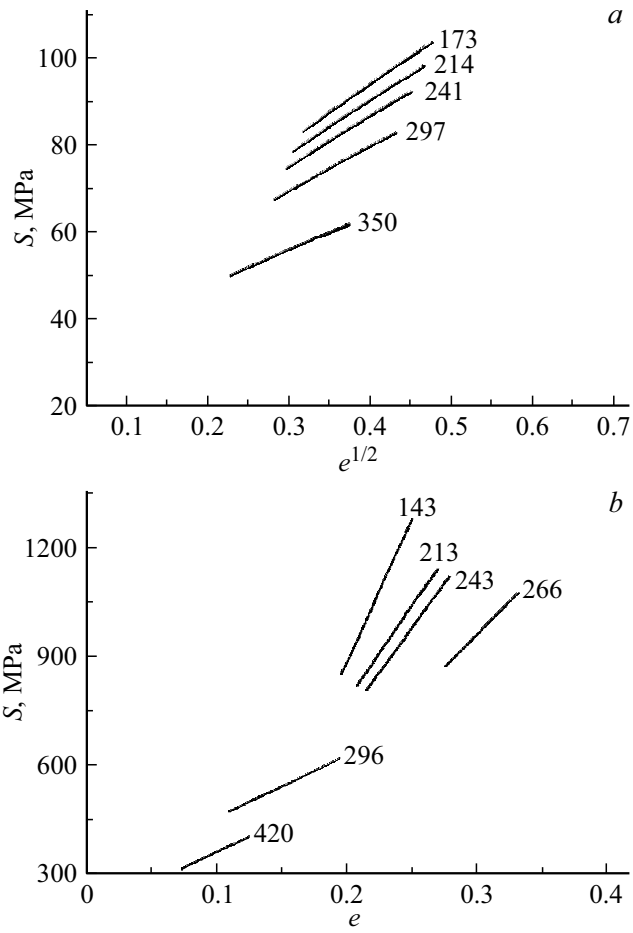

Figure 2. Distinguishing the stages of parabolic strain hardening in aluminum (a) and linear strain hardening in austenite (b) at different temperatures.

The pattern of localized plasticity was visualized by the method of two-exposure digital speckle photography [1], with the help of which the fields of displacement vectors on the sample surface $\mathbf{r}(x, y)$ were reconstructed. Then the local deformations were calculated, i. e. vector field gradient components (plastic distortion tensor) $\beta_{i,j} = \nabla \mathbf{r}(x, y)$ [4]. Knowing these components at all points of the sample surface, it was possible to construct their distributions $\varepsilon_{ij}(x, y)$, which *in situ* visualize the pattern of localized plasticity for different moments of time. In this case, it becomes possible to monitor the pattern evolution (change of autowave modes) of localized plasticity in real time.

The numerical values of the kinematic autowave characteristics of the localized plasticity λ and V_{aw} were measured from the Xt-diagrams (X — coordinate of the local deformation center, t — time) plotted from distribution analysis data for any of the components of the plastic distortion tensor, as shown in Fig. 3. The method for measuring the length λ and the period T_t of localized plasticity autowave is also explained here.

2. Autowave interpretation of the temperature effect of plasticity

As follows from Fig. 4, the temperature effect on the flow curves is reduced to the fact that with its growth, the yield strength and ultimate strength decrease, while plasticity increases. The authors [5] explained the extreme temperature behavior of the elongation to fracture of austenite at ~ 320 K by the fact that the strain hardening at large strains is higher than the flow stresses.

The input data show that upon with temperature change there are practically no qualitative differences in the change of the deformation characteristics of the two studied metals. Only certain quantitative differences are observed, obviously related to the different nature of the dislocation deformation mechanisms that control the processes in these cases [3]. It can be said that the temperature effect on the nature of the flow curves and the strength characteristics of the studied metals is practically indistinguishable.

Physically more meaningful is such mechanical characteristic as the strain hardening coefficient $\theta = ds/de$ [3]. The

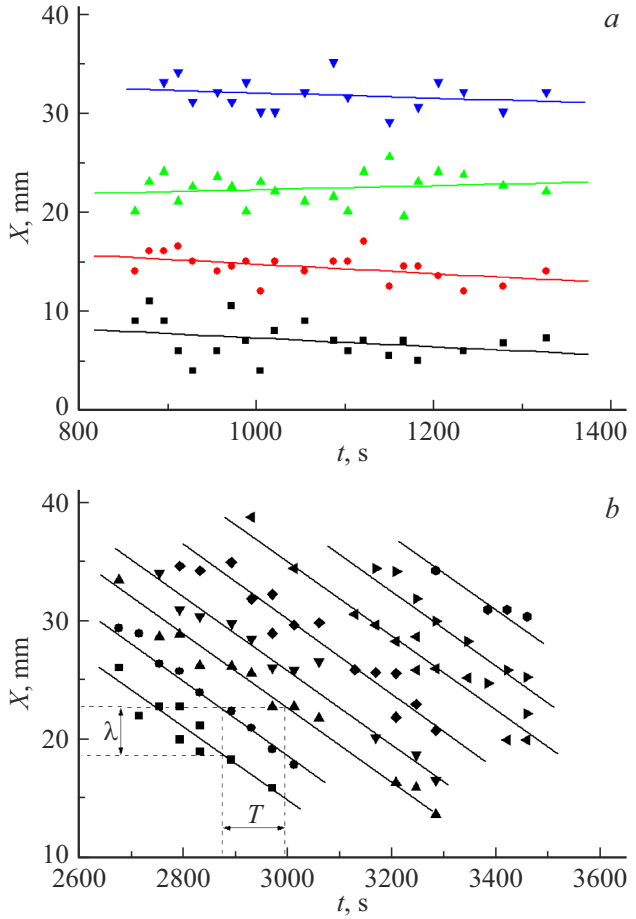

Figure 3. $X-t$-diagrams for the autowave plasticity of the investigated metals. Stationary dissipative structure in aluminum at the stage of parabolic strain hardening (a) and a phase autowave in austenite at the stage of linear strain hardening (b). Temperature is 300 K.

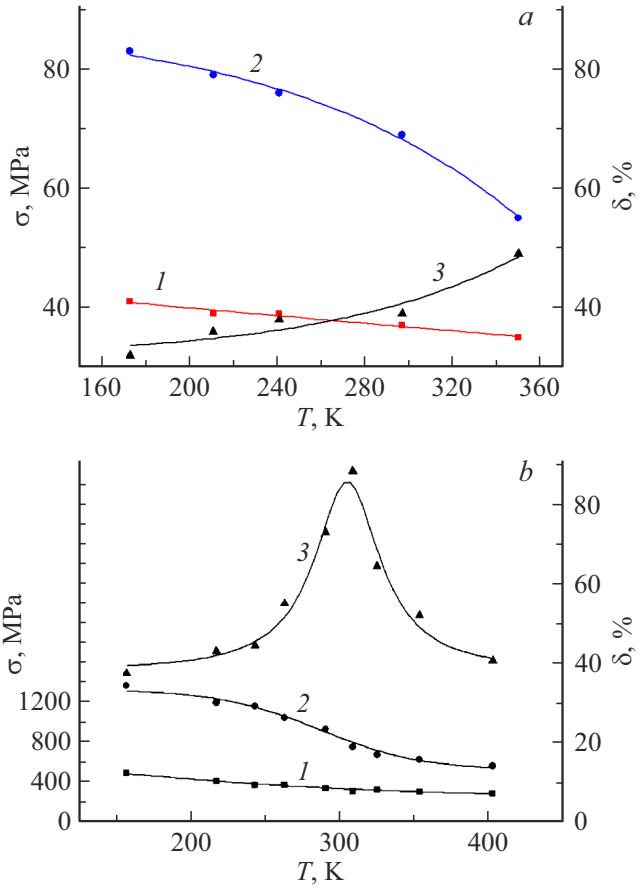

Figure 4. Temperature dependences of the mechanical properties of aluminum (a) and austenite (b). *1* — yield strength, *2* — tensile strength, *3* — contraction at break.

temperature dependence of this variable for the cases of deformation of aluminum and austenite is shown in Fig. 5. For both metals, the relation is valid

$$\theta = \theta_0 \exp\left(\frac{Q}{k_B T}\right), \qquad (2)$$

where k_B is the Boltzmann constant and $\theta_0 = \text{const}$. The activation energies of the strain hardening coefficient Q are $Q^{(\text{Al})} \approx 0.015$ eV and $Q^{(\text{aust})} \approx 0.02$ eV.

The analogy in the deformation characteristics behavior of aluminum and austenite is quite interesting, however, when using the concepts of the autowave model of plasticity, significant differences in the temperature effects for the two studied metals are revealed. This is indicated, in particular, by the different form of the $X-t$-diagrams for the stationary dissipative structure in aluminum and the phase autowave of localized deformation in austenite shown in Fig. 3, a and it b respectively. Such forms of $X-t$-diagrams mean that in the case of aluminum deformation, a stationary dissipative structure is formed in the material. In this structure, the centers of localized plasticity are fixed; $V_{aw} = 0$. Under the same deformation conditions, at the stage of linear strain hardening a phase autowave of localized plasticity is formed

in austenite, which is characterized by the autowave length λ and its propagation speed $V_{aw} \neq 0$. The variables λ and V_{aw} can be found independently, as shown in Fig. 3, *b*.

In addition to the difference in the form of $X-t$-diagrams, one should also note the fundamental difference in temperature responses during deformation of aluminum and austenite. As follows from Fig. 6, *a*, when a stationary dissipative structure appears at the stage of parabolic strain hardening of aluminum $\ln(\lambda) \propto T^{-1}$, i. e. with rise of the test temperature, the length of the localized plasticity autowave decreases. In this case, as follows from Fig. 3, *a*, for stationary dissipative structure $V_{aw} = 0$. In the same temperature range, during the formation of the phase autowave at the stage of linear strain hardening of austenite, in accordance with Fig. 6, *b*, the autowave propagation speed increases exponentially with temperature rise according to the law $\ln(V_{aw}) \propto T^{-1}$, but according to Fig. 3, *b*, $\lambda = \text{const}$.

This means that different autowave characteristics are temperature-dependent at the stages of parabolic and linear strain hardening (in aluminum and austenite, respectively). Plasticization with test temperature increasing is associated in the first case (aluminum) with decrease in length of the autowave of localized plasticity, and in the second case

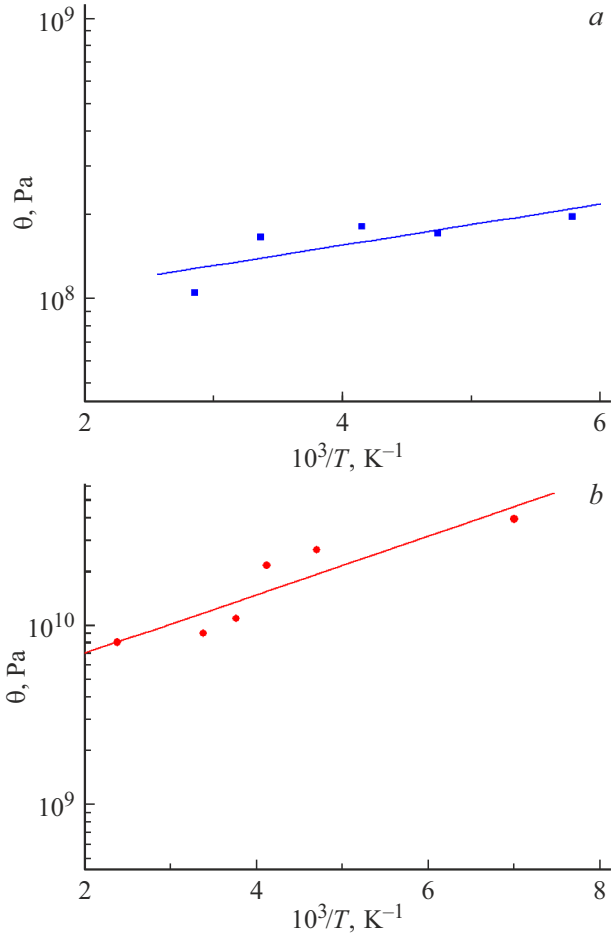

Figure 5. Temperature dependences of the strain hardening coefficient of aluminum (*a*) and austenite (*b*).

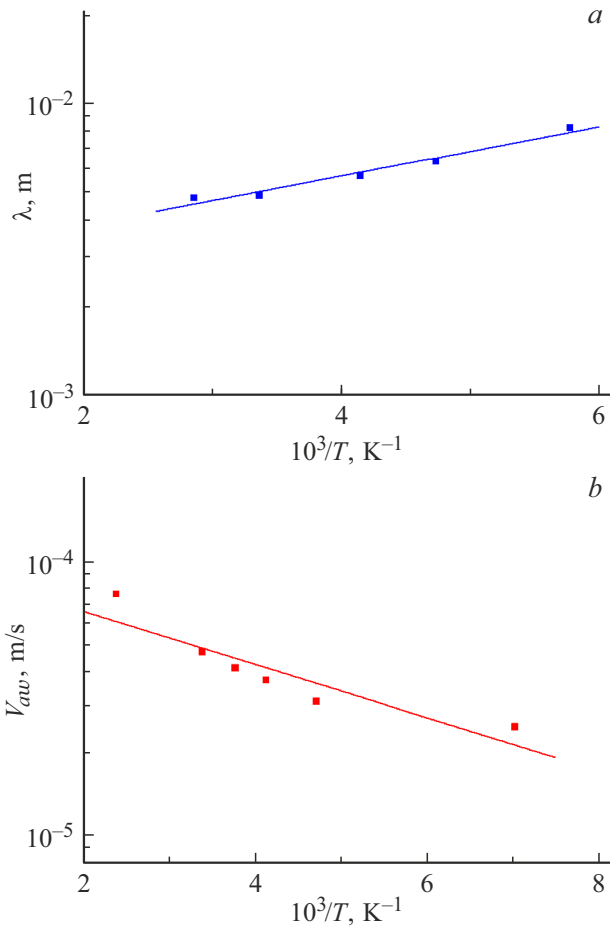

Figure 6. Temperature dependence of autowave characteristics for deformation of aluminum (*a*) and austenite (*b*).

(austenite) — with increase in the propagation speed of phase autowaves of localized plasticity.

It seems a promising attempt to relate the explanation of the nature of the temperature dependence of the strain hardening coefficients for aluminum and austenite, given by equation (2), with the temperature dependences of the autowave characteristics $\lambda(T)$ and $V_{aw}(T)$, shown in Figs. 6. Analyzing Fig. 6, *b*, we note that, as mentioned above, $V_{aw} = \lambda/T_t = (2\pi)^{-1}\lambda\omega_{aw}$, where $\omega_{aw} = 2\pi/T_t$ — frequency of the phase autowave. For $\lambda = \text{const}$ this corresponds to the well-known relation for the frequency of thermally activated events [6,7]:

$$\omega_{aw} = \omega_D \exp\left[\frac{H(\sigma)}{k_B T}\right]. \qquad (3)$$

Here $H \approx U - \gamma\sigma$ — activation enthalpy, U — potential barrier height, γ — activation volume [6], and ω_D — Debye frequency. From Fig. 6, *b* it follows that $U^{(\text{aust})} \approx 0.02$ eV, and $\gamma \approx 8.5b^3$, where $b \approx 0.2$ nm is the Burgers vector of dislocations in austenite. The coincidence of the values $Q^{(\text{aust})}$ and $U^{(\text{aust})}$ for the case of austenite deformation makes it possible to explain the temperature dependence of the strain hardening coefficient at the stage of linear

strain hardening (Fig. 5) by the temperature dependence of the propagation speed of the phase autowave of localized plasticity.

The last provision needs to be clarified. As was established earlier [1], at the stage of linear strain hardening, the propagation speed of the phase autowave of localized deformation is given by the relation $V_{aw} \approx \Xi/\theta$, in which the experimentally determined constant $\Xi \approx 5 \cdot 10^{-7}$ m/s [1,2]. Then, for the strain hardening coefficient, we can write

$$\theta = \frac{\Xi}{V_{aw}} \sim V_{aw}^{-1}. \qquad (4)$$

The numerical estimate of the dimensionless coefficient θ gives $\theta \approx 3 \cdot 10^{-3}$, which is close to the experimentally observed values [8–10]. Taking into account the temperature dependence of the autowave speed given by equation (3), the strain hardening coefficient at the linear stage of the process has the form

$$\theta(T) \approx \Xi[V_{aw}(T)]^{-1} = 2\pi \frac{\Xi}{\lambda\omega_D} \exp\left[\frac{U - \gamma\sigma}{k_B T}\right], \qquad (5)$$

where the length of the autowave is $\lambda = \text{const}$.

The dependence $\ln(\lambda) \propto T^{-1}$ for aluminum basically behaves in the same way, and the corresponding calculations for aluminum, performed using the data in Fig. 6, *a*, lead to the potential barrier height $U^{(\text{Al})} \approx 0.017$ eV and $\gamma \approx 12.3b^3$, where $b \approx 0.286$ nm is the Burgers vector of dislocations in Al. The values of $Q^{(\text{Al})}$ and $U^{(\text{Al})}$ obtained for the deformation of aluminum, as well as for the deformation of austenite, practically coincide, which allows us to consider the temperature dependence of the autowave length as the cause of temperature dependence of the strain hardening coefficient at the parabolic stage of hardening.

However, it is known from the theory of thermally activated processes [6] that the linear characteristic (scale) λ cannot be considered as a thermally activated value. In other words, one should assume the existence of a temperature-dependent parameter that during deformation would be „linked“ with the scale λ, ensuring its exponential decrease with temperature rise. As such a parameter it is natural to use the probability of cross slip events.

It is known that in aluminum this type of dislocation slip develops from the very beginning of plastic flow, providing a parabolic shape of the flow curve [11,12]. Transverse slip is based on the ejection of helical dislocation loops into an inclined slip plane in a crystal. The probability of such events is determined by the relation $p \propto \exp(-W_{cs}/(k_B T))$, where W_{cs} — the height of the energy barrier for such a burst [6]. This probability increases with temperature rise, which, accordingly, indicates the frequency increasing of nucleation of new deformation centers. As a result, this causes a decrease in the autowave length of localized plasticity during the formation of a stationary dissipative structure at the stage of parabolic strain hardening. Autowave effects during plastic deformation were also observed and discussed in [13–16].

Conclusion

In this paper the thermally activated change in plasticity indices in metals with FCC lattice was experimentally studied. The numerical values of the activation parameters of deformation are estimated in the case of the appearance of stationary dissipative structures during parabolic strain hardening and in the case of generation of phase autowaves at the stage of linear strain hardening.

A functional relationship between the macroscopic deformation characteristic — the strain hardening coefficient — and the autowave parameters of the localized plasticity pattern is found. The nature of the relationship for parabolic and linear strain hardening is different. Thus, during parabolic hardening temperature changes in the strain hardening coefficient are associated with changes in the autowave length of the localized plasticity, while during linear strain hardening they are controlled by changes in the speed of its propagation.

Funding

The paper was prepared as part of the state assignment of the Institute of Strength Physics and Materials Science of the Siberian Branch of the Russian Academy of Science, subject № FWRW-2021-0011.

Conflict of interest

The authors declare that they have no conflict of interest.

References

[1] L.B. Zuev, S.A. Barannikova. Crystals, **9**, 458 (2019). DOI: 10.3390/cryst9090458
[2] L.B. Zuev. In: *Multiscale Biomechanics and Tribology of Inorganic and Organic Systems*, ed. by G.-P. Ostermeyer, V.L. Popov, E.V. Shilko, O.S. Vasiljeva (Springer, Berlin, 2021), p. 245. DOI: 10.1007/978-3-030-60124-9_12
[3] J. Pelleg. *Mechanical Properties of Materials* (Springer, Dordrecht, 2013)
[4] A. Kadich, D. Edelen. *Kalibrovochnaya teoriya dislokatsij i disklinatsij* (Mir, M., 1987) (in Russian)
[5] N. Tsuchida, Y. Morimoto, T. Tonan, Y. Shibata, K. Fukaura, R. Ueji. ISIJ Int., **51**, 124 (2011). DOI: 10.2355/isijinternational.51.124
[6] D. Caillard, J.L. Martin. *Thermally Activated Mechanisms in Crystal Plasticity* (Elsevier, Oxford, 2003)
[7] L.B. Zuev, Y.A. Khon, Phys. Mesomech., **25** (2), 103 (2022). DOI: 10.1134/S1029959922020011
[8] G.A. Malygin. Phys. Sol. St., **48** (4), 693 (2006) DOI: 10.1134/S1063783406040123
[9] J.S. Langer, E. Bouchbinder, T. Lookman. Acta Mater., **58** (12), 3718 (2010). DOI: 10.1016/j.actamat.2010.03.009
[10] A. Ishii, J. Li, S. Ogata. Int. J. Plast., **82**, 32 (2016). DOI: 10.1016/j.ijplas.2016.01.019
[11] I. Kovács, N.Q. Chinh, E. Ková cs-Csetényi. Phys. Stat. Sol. A, **17** (7), 3 (2002). DOI: 10.1002/1521-396X

[12] P. Landau, R.Z. Shneck, G. Makov, A. Venkert. Mater. Sci. Eng., **3**, 012002 (2009). DOI: 10.1088/1757-899X/3/1/012004
[13] A. Asharia, A. Beaudoin, R. Miller. Math. Mech. Sol., **13**, 292 (2008). DOI: 10.1177/1081286507086903
[14] R.J. McDonald, C. Efstathiou, P. Kurath. J. Eng. Mater. Technol., **131**, 652 (2009). DOI: 10.1115/1.3120410
[15] C. Fressengeas, A. Beaudoin, D. Entemeyer, T. Lebedkina, M. Lebyodkin, V. Taupin. Phys. Rev. B, **790**, 14108 (2009). DOI: 10.1103/PhysRevB.79.014108
[16] M.A. Lebyodkin, N.P. Kobelev, Y. Bougherira, D. Entemeyer, C. Fressengeas, V.S. Gornakov, T.A. Lebedkina, I.V. Shashkov. Acta Mater., **60**, 3729 (2012). DOI: 10.1016/j.actamat.2012.03.026